The expression of cockroach insulin-like peptides is differentially regulated by physiological conditions and affected by compensatory regulation

Júlia Castro-Arnau, Ainoa Marín, Marc Castells, Iamil Ferrer and José L. Maestro*

Institute of Evolutionary Biology (CSIC-Universitat Pompeu Fabra), Passeig Marítim de la Barceloneta 37-49, 08003 Barcelona, Spain.

*Corresponding author (email address: joseluis.maestro@ibe.upf-csic.es)

Keywords: insulin-like peptide; juvenile hormone; vitellogenin; insect, *Blattella germanica*; nutritional signaling

ABSTRACT

In insects, the insulin receptor (InR) pathway is involved in regulating key physiological processes, including juvenile hormone (JH) synthesis, vitellogenin production, and oocyte growth. This raises the question about which ligand (or ligands) binds to InR to trigger the above effects. We have cloned seven insulin-like peptides (*BgILP1* to *7*) from female *Blattella germanica* cockroaches and found that the brain expresses *BgILP1* to *6*, the fat body *BgILP7*, and the ovary BgILP2. Starvation induces the reduction of *BgILP3*, 5, and *6* mRNA levels in the brain, and the various *BgILPs* are differentially expressed during the gonadotrophic cycle. In addition, by knocking down the BgILPs we were able to identify compensatory regulation at transcriptional level between the different BgILPs, although none of the BgILP knockdown assays, including the knockdown of the seven BgILPs, produced the same phenotypes that we achieved by depleting InR. Taken together, the results indicate that *B. germanica* ILPs are differentially expressed in tissues and in response to physiological conditions, and that they are affected by compensatory regulation.

Introduction

The insulin/insulin-like growth factor signaling (IIS) pathway is involved in key physiological processes, such as growth, cell proliferation, metabolism, longevity, reproduction, and insect caste determination (Claeys et al., 2002; Wu and Brown, 2006). Its activity is triggered by binding a ligand (insulin or related molecules) to a membrane receptor (insulin receptor (InR) or insulin-like growth factor-1 (IGF-1) receptor) together with the molecular response this binding induces in the cells (Claeys et al., 2002; Wu and Brown, 2006). Thus, the activity of the InR pathway can be modified by modulating the synthesis and release of the ligands in the endocrine organs that synthetize them and by regulating the pathway in the target cell.

In insects, the first insulin orthologue was purified from the silkworm, *Bombyx mori* (Nagasawa et al., 1984), and, since then, insulin-like peptides (ILPs) have been identified in many insect species from different orders. The number of ILPs varies greatly depending on the species, ranging between one peptide in locusts (Badisco et al., 2008; Lagueux et al., 1990) and 37 peptides in *B. mori* (Aslam et al., 2011). ILPs are the putative ligands of insect InR, although at least *Drosophila melanogaster* dilp8 binds to the leucine-rich repeat-containing G protein-coupled receptor Lgr3 (Colombani et al., 2015; Garelli et al., 2015; Vallejo et al., 2015)

With regard to the function of the InR pathway in reproduction, in *D. melanogaster*, a hypomorphic mutation of InR induces reduced juvenile hormone (JH) synthesis in adult females, and the ovaries remain immature (Tatar et al., 2001). In the mosquito *Aedes aegypti*, activating the InR pathway with bovine insulin promotes an increase in JH synthesis and vitellogenin (*Vg*) expression, whereas decreased activity of the InR pathway produces reduced JH synthesis, together with lower levels of the enzymes of the JH biosynthesis pathway and less Vg (Gulia-Nuss et al., 2011; Perez-Hedo et al., 2014; Pérez-Hedo et al., 2013; Roy et al., 2007).

In the German cockroach, *Blattella germanica*, RNAi-triggered knockdown of InR and starvation produce, in both cases, reduced JH synthesis, concomitant with a decrease in 3-hydroxy-3-methylglutaryl coenzyme A (HMG-CoA) synthase-1 and -2, HMG-CoA reductase, JH acid methyltransferase (JHAMT), and methyl farnesoate epoxidase (Abrisqueta et al., 2014; Dominguez and Maestro, 2018). In addition, the treatments induce decreased *Vg* expression, at least in part independent of JH action, and less yolk is deposited in the developing follicle (Abrisqueta et al., 2014).

In this work we identified the putative InR ligands (ILPs) from *B. germanica*, studied their expression and, by knocking them down, either individually or collectively, we tried to recover a similar phenotype as we found with InR knockdown. The results showed differential expression of the seven *B. germanica* ILPs (*BgILPs*) identified, both at temporal

and tissue levels, as well as in response to starvation. In addition, we identified compensatory transcriptional regulation between different BgILPs. However, none of the BgILP knockdown assays, including the knockdown of the seven BgILPs, produced the same phenotypes in terms of expression of JH biosynthesis enzymes, *Vg,* or ovary development, that we achieved by depleting InR.

Material and Methods

Insects

Specimens of *B. germanica* were obtained from a colony reared on dog food and water at 30 ± 1 °C and 60-70 % relative humidity. Dissections of brains, corpora allata-corpora cardiaca (CC-CA), fat bodies and ovaries from adult females were carried out in Ringer's saline on carbon dioxide-anesthetized specimens. For the starvation assays, animals received only water after the imaginal moult. In the case of the quantification of the ILPs expressions in the different tissues and in fed vs. starved animals, 5-day old females in the first gonadotrophic cycle were used. For the RNAi treatments, females in the fifth day of the second gonadotropic cycle were used.

RNA extraction, cDNA synthesis and quantitative real-time PCR analysis

cDNAs were synthetized from total RNA as previously described (Abrisqueta et al., 2017; Maestro et al., 2009). In the case of fat bodies or ovaries, 1 µg of total RNA was used, whereas in the case of brain or CC-CA, the whole RNA amount extracted from the sample was used. The absence of genomic contamination was confirmed using a control without reverse transcription. Quantitative real-time PCR analysis were carried out as described previously (Maestro et al., 2009). Primer sequences to amplify the different *BgILPs* and *HMG-CoA reductase* are provided in Table S1. The primers used to amplify *HMG-CoA synthase-1*, *JHAMT*, *Vg*, *InR*. *Actin 5C* (used as a reference) have been reported elsewhere (Abrisqueta et al., 2014; Dominguez and Maestro, 2018; Ons et al., 2015; Süren-Castillo et al., 2012). GenBank accession numbers for all the genes analyzed in the present work are indicated in Table S2. The total reaction volume was 20 µL. All reactions were run in duplicate or triplicate. The results are expressed as copies of a specific mRNA per copies of *Actin 5C*.

RNA interference *in vivo*

Systemic RNAi treatments were performed as previously described (Dominguez and Maestro, 2018; Maestro et al., 2009), with some modifications. The primers used to generate the different dsRNAs for the RNAi treatments against the different BgILPs are described in Table S3. For avoiding the possible effects of protein depletion during nymphal development, we decided to treat adult females. In the case of a single dsRNA treatment, 2

µg were injected into the abdomen of adult females in the first day of ootheca transport, and the treatment was repeated 7 days later. In the case of the triple treatment, this consists on the injection of 2 µg of dsILP3 the first day of oothecal transport, 2 µg dsILP5 on day 4th and 2 µg dsILP6 on day 7th. In the case of the treatment designed for knocking down all seven BgILPs, the treatment was 2 µg of dsILP2 and dsILP3 on the first day, 2 µg dsILP1 and dsILP5 on day 4th, 2 µg dsILP7 on day 6th and 2 µg dsILP4 and dsILP6 on day 8th. In all cases, oothecae were removed on the twelfth day of its transport, which induced the onset of the second gonadotrophic cycle, and dissections were made at the fifth day of the second gonadotrophic cycle which is, in all aspects, perfectly comparable to the first gonadotrophic cycle. A heterologous 307 bp fragment from the gene sequence of the polyhedrin of *Autographa californica* nucleopolyhedrovirus was used as negative control and injected following the same treatment protocols. Mortality induced by RNAi treatments was totally negligible.

Immunohistochemistry

To generate antisera specific for BgILP5, a peptide corresponding to the amino acids 52-62 of BgILP5 sequence (CNGRYYTPDED) localized in the B-chain, was used as immunogen. The peptide was conjugated with horseshoe crab hemocyanin. The preparation of the antisera was performed by the Custom Antibody Service (CAbS), a platform of CIBER-BBN (Biomedical Research Networking center in Bioengineering, Biomaterials and Nanomedicine), which forms part of the Spanish Research Council (IQAC-CSIC), with the support of the ICTS NANBIOSIS.

Adult female brains were dissected, fixed in paraformaldehyde (4% in PBS) for 1 h at room temperature, washed three times with PBT (PBS, 1% Triton-X100) and blocked with PBTBN (PBT, 1% BSA and 10% normal goat serum) for 1 h at room temperature. They were then incubated overnight at 4ºC with the primary anti-BgILP5 antiserum diluted 1:20000 in PBTBN. After PBT washing, tissues were incubated for 2 h with Alexa-Fluor 647 conjugated donkey anti-rabbit (Life Technologies) at 1:400 in PBTBN. In addition, tissues were incubated at room temperature for 5 min in 1 µg/ml DAPI (Sigma) in PBT. After PBT washing, tissues were mounted in Mowiol (Calbiochem, Madison, WI, USA) and observed using a Zeiss AxioImager Z1 microscope (Apotome) (Carl Zeiss MicroImaging).

The specificity of the antiserum was checked by comparing total signal with the signal produced with the antiserum blocked overnight with an excess of the immunogenic peptide (5 µl peptide at 1mg/ml + 5 µl undiluted antiserum). In addition, we compared the signal obtained by the anti-BgILP5 antiserum in brains from control and dsILP5-treated females.

Statistical analysis

Statistical analyses were performed using IBM SPSS Statistics 24. In the case of the analysis of expression through the gonadotrophic cycle, one-way ANOVA with HSD (honestly-significant-difference) Tukey's test was performed. For the remaining experiments, comparison of results from control and treated animals was performed using Student's *t*-test.

Results

B. germanica has seven ILP genes

Combining a BLAST search of *B. germanica* transcriptomes (Ylla et al., 2018) with the analysis of a draft version of this cockroach's genome (Harrison et al., 2018) (https://www.hgsc.bcm.edu/arthropods/german-cockroach-genome-project) and PCR strategies, we obtained the sequences of 7 independent cDNAs showing the characteristic ILP structure: signal peptide-B chain-C peptide-A chain, and the conserved amino acids, particularly cysteines, that provide the "insulin-like" structure. After extensive searching, no further sequences were identified, for which reason we assume these 7 represent the ILP orthologues in *B. germanica*. Due to the difficulty of identifying orthologies between the different ILPs that do not belong to closely related species (Antonova et al., 2012; our own results, not shown), the BgILPs were numbered according to the order they were identified in, without taking into account the names of ILPs described for other species.

The *BgILP1*, *2*, *3*, *4*, *5* and *6* sequences were obtained from the transcriptomes, and then the full-length cDNA sequences were identified (Fig. 1). In the case of *BgILP7*, the whole open reading frame sequence was retrieved from the genome, and the 5'-UTR was obtained by 5'-RACE. For all the sequences, at least the open reading frames were verified through PCR, cloning, and sequencing. The corresponding GenBank accession numbers are indicated in Table S2. All seven sequences code for a signal peptide (identified by SignalP 4.1 (Petersen et al., 2011)), which indicates that they will be secreted, and for the characteristic cysteines that facilitate the folded insulin structure. For BgILP1 to BgILP6, we identified mono- and dibasic sites that show a high probability of being proteolytic enzyme targets (Veenstra, 2000), thus producing a final molecule consisting of two different peptides bound by disulfide bonds. For the site after the C-peptide in BgILP1 and BgILP2, we chose the single Arg, instead of the Arg-Arg site, because this dipeptide is not always used in insects, whereas a single Arg with another Arg in the -4 position is prone to be used as a cleavage site (Veenstra, 2000). Although the cleavage site Lys-Lys is quite rare (Veenstra, 2000), we counted it as an active site because the same dipeptide in the same position is used in locust insulin-related peptide (IRP) (Badisco et al., 2008). In the case of BgILP7, the presence of an aliphatic amino acid (Val) after the Arg-Arg dipeptide at the end of the B-chain could inactivate this dibasic site and make the cleavage less probable

(Veenstra, 2000). For this reason, we consider that BgILP7 could be released as a single chain.

BgILPs are differentially expressed in tissues and through the gonadotrophic cycle

The mRNA levels of the seven BgILPs were checked in the brain, corpora cardiaca (CC), corpora allata (CA), fat body, ovary, and midgut of 5-day-old adult females of *B. germanica* (Fig. 2). The results show that whereas *BgILP1* to *BgILP6* are expressed in the brain, *BgILP7* mRNA levels were much lower in this organ, close to the detection limit. *BgILP1* mRNA and also *BgILP2* mRNA (although at lower levels), were found in the CC and CA. The fat body expresses mainly *BgILP7* and, to a lesser extent, *BgILP2*. *BgILP2* is the only mRNA found in the ovaries, whereas none of the seven *BgILP* mRNAs were found in the midgut.

Using a polyclonal antibody designed against a peptide corresponding to the amino acids 52-62 located in the B chain of the BgILP5 protein sequence, we localized a group of 5-6 immunoreactive insulin-producing cells (IPCs) found in each brain hemisphere, in the pars intercerebralis of the protocerebrum (Fig. 3A). This signal disappeared when we utilized the antisera blocked with an excess of the peptide used for the immunization (results not shown). IPC staining disappears in the brains of females treated with dsRNA against BgILP5 (Fig. 3B).

In addition, *BgILP* mRNA levels were measured in the various tissues on different days throughout the first gonadotrophic cycle. The days were selected as representative of diverse physiological and gonadotrophic conditions, as follows: day 1 - previtellogenesis; day 3 - early vitellogenesis; days 5 and 6 - full vitellogenesis; day 7 - end of vitellogenesis. In the case of the brain, whereas *BgILP3* and *BgILP5* (and to a lesser extent *BgILP6*) follow an expression pattern approximately parallel to that of vitellogenesis, those of *BgILP1*, *BgILP2* and *BgILP4* present flatter profiles (Fig. 4). *BgILP2* mRNA levels in the ovary and *BgILP7* mRNA levels in the fat body decrease and increase, respectively, throughout the gonadotrophic cycle (Fig. S1).

Starvation differentially regulates *BgILP* expression

To elucidate the effect of nutrition on *BgILP* expression we compared *BgILP* mRNA levels between 5-day-old control-fed females and females of the same age that had been starved since the imaginal molt. Starvation did not affect mRNA levels of *BgILP1*, *BgILP2* and *BgILP*4 in the brain, but did produce a 53% reduction in *BgILP6* mRNA levels and a 90% reduction in *BgILP3* and *BgILP5* mRNA levels (Fig. 5A). *BgILP7* mRNA levels in the fat body showed an 88% decrease in starved females (Fig. 5B), whereas ovary *BgILP2* mRNA levels showed a ca. 7-fold increase in starved, compared to fed females (Fig. 5C).

Effect of BgILP knockdown on *BgILP* expression, JH synthesis and vitellogenesis

To elucidate the BgILP (or BgILPs) responsible for activating JH synthesis and vitellogenesis in response to adequate nutrition, we performed a dsRNA-triggered knockdown of each BgILP and analyzed *BgILP* mRNA levels as well as the expression of key enzymes in the JH biosynthetic pathway in CA and *Vg* in the fat body.

Single RNAi knockdown of each BgILP (dsILP1 to dsILP7) produced a specific reduction in mRNA levels of the targeted BgILP (greater than 90% in the case of the brain and ca. 66% for fat body BgILP7), without affecting the expression levels of the other BgILPs, except in the case of the dsILP5 treatment and, to a certain extent, the dsILP3 treatment (Figs. 6A, 7A, S2A, S3A, S5A, S7A, and S8A). Thus, treatment with a dsRNA targeting *BgILP5* (dsILP5) produced a 75% increase in the mRNA levels of *BgILP3* (Fig. 7A). In addition, dsILP3 treatment produced a 76% increase in *BgILP5* mRNA levels, although the increase was not statistically significant (Fig. 6A). Nevertheless, none of the treatments reduced the expression of the key enzymes in JH biosynthesis, *HMG-CoA synthase-1*, *HMG-CoA reductase*, or *JHAMT*, in the CA, and just a 1.7-fold increase in *JHAMT* mRNA for dsILP3 was observed (Figs S2 to S8). In addition, none of the treatments produced modifications of *Vg* expression or changes in the growth of developing follicles, with the exception of a low, although statistically significant, reduction in basal follicle length in the case of dsILP5 (Figs 7 and S2 to S8).

Once we checked that single BgILP depletion did not affect the tested reproductive parameters, we wondered whether the different BgILPs might have redundant functions. We therefore checked the effect of depleting the brain BgILPs, whose expression was lower in starved vs. fed females (*BgILP3*, *BgILP5* and *BgILP6*), under the hypothesis that these low levels could cause the reduced expression of JH biosynthesis enzymes and *Vg* observed during starvation (Dominguez and Maestro, 2018; Maestro et al., 2009). The triple knockdown produced a greater than 95% depletion of the targeted *BgILP* mRNAs, without affecting the expression of the other *BgILPs* (Fig. S9). Nevertheless, the expressions of *HMG-CoA synthase 1*, *HMG-CoA reductase*, and *JHAMT* in the CA, and *Vg* in the fat body were unaffected (Fig. S9).

Finally, we decided to try to deplete the expression of all seven *BgILPs* identified, with the idea of replicating the phenotype observed when depleting InR. To do this, we injected the corresponding dsRNAs targeting the seven BgILPs (dsILP1-7), and measured their expressions. The results revealed a significant and substantial reduction in the mRNA levels of all seven *BgILPs* (around 90% in the case of brain *BgILPs* (Fig. 8A) and 80% in fat body *BgILP7* (Fig. 8C)), but again no changes were observed in the JH biosynthesis enzymes in CA, or *Vg* in the fat body (Fig. 8B and C). This result led us to consider the hypothesis that depleting the BgILPs would result in increased *InR* expression in the CA, as a compensatory feedback. Nevertheless, no changes were observed in CA *InR* mRNA levels in treated compared to control females (Fig. 8B).

Discussion

In *B. germanica*, starvation and RNAi-triggered knockdown of InR dramatically reduces adult female JH and Vg synthesis (Abrisqueta et al., 2014; Dominguez and Maestro, 2018). Furthermore, knockdown of the transcription factor FoxO, the main transcriptional effector of the InR pathway, partially reverts the reduction of JH and Vg in starved females (Süren-Castillo et al., 2012). These results suggest that, in a situation involving adequate nutritional input, the InR pathway would be activated and, in turn, this would activate JH synthesis and Vg production. InR is a membrane receptor that must, presumably, be activated by the binding of its ligands (Claeys et al., 2002). The next question is which InR ligand (or ligands) is involved in activating InR and the reproductive processes in the adult female in response to nutrition? The search for InR ligands provided the sequences of seven *B. germanica* ILPs (BgILP1 to BgILP7) with the characteristic insulin structure.

The amino acid sequences of the BgILP1, 2, 3, 4, 5, and 6 propeptides suggest that these would cleave between the B-chain and C-peptide and between the C-peptide and the A-chain, whereas BgILP7 would be released as a single chain (Veenstra, 2000). This would make BgILP7 more similar to IGF than to insulin. In addition, BgILP7 is the BgILP with the shortest C-peptide and the longest C-terminal sequence, these two facts being more characteristic of IGFs than of insulins (Humbel, 1990). In the silkworm, *B. mori*, one peptide (BIGFLP), mainly synthesized in the fat body and purified from the hemolymph as a single chain, is considered similar to IGF (Okamoto et al., 2009a). Also, in *D. melanogaster*, dilp6, mainly expressed in the fat body, is considered to be the fly's IGF (Okamoto et al., 2009b; Slaidina et al., 2009). Interestingly, the tissue that predominantly expresses BgILP7 is also the fat body. None of the BgILPs show the two Arg (or Arg + Lys) in N and N + 4 positions between the two Cys of the B-chain, characteristic of relaxin-type peptides (Patil et al., 2017).

BgILP2, BgILP3, and BgILP4 show a sequence between the signal peptide and the B-chain that has certain similarities with an IRP copeptide identified from locust CC, located in the same position in the locust prepropeptide for insulin-related peptide (IRP), and which has been demonstrated to cause a decrease in glycogen phosphorylase activity in locusts (Clynen et al., 2003). The occurrence of these peptides in *B. germanica,* and their effect on glycogenolysis is worth pursuing in subsequent studies. Similarly, the occurrence of the *B. germanica* C-peptides and assaying their possible activity (Bermudez et al., 1991) is beyond the scope of this work.

With regard to tissue expression, the adult female brain expresses *BgILP1*, *2*, *3*, *4*, *5*, and *6*, whereas in fat bodies we mainly found *BgILP7* mRNA. The ovaries only express

BgILP2 and we found no BgILP expression in the midgut. *BgILP1* mRNA was also detected in CC and CA. Although we cannot totally rule out the possibility that these mRNAs were synthesized in CC or CA cells, we consider that the *BgILP* mRNAs present in these organs must be synthetized in brain cells and transported along their axons to their release areas, as, to date, the synthesis of ILP in the glandular part of the CC or in the CA has not been described in any species. CC and CA function as neurohemal releasing areas and the occurrence of ILPs in axons terminating in these glands have been described in various species from different insect orders, including *D. melanogaster* (Géminard et al., 2009; Rulifson et al., 2002), *A. aegypti* (Riehle et al., 2006), *Anopheles gambiae* (Krieger et al., 2004), *Spodoptera littoralis* (Van de Velde et al., 2007), and *Schistocerca gregaria* (Badisco et al., 2008). Differential ILP expression in tissues and in developmental stages has been reported in several species, including *D. melanogaster* (Brogiolo et al., 2001; Broughton et al., 2008; Ikeya et al., 2002; Okamoto et al., 2009b; Slaidina et al., 2009; Veenstra et al., 2008), *A. aegypti* (Riehle et al., 2006), and *Nilaparvata lugens* (Lu et al., 2018).

In order to determine the sites of synthesis of the BgILPs in the brain, we carried out an immunohistochemical study using an antiserum against BgILP5. This analysis led to the identification of 5-6 immunoreactive cells (IPCs) in each lobe of the pars intercerebralis of the brain in adult *B. germanica* females. This labelling appears to be specific, since it disappears when the antiserum is blocked with the antigen and in dsILP5-treated animals. This group of IPCs has been identified in all the insects in which it has been sought (Badisco et al., 2008; Broughton et al., 2005; Riehle et al., 2006; Van de Velde et al., 2007). Although we did not follow the complete path of the immunoreactive axons emerging from *B. germanica* IPCs, we assume that these would reach the neurohemal areas of CC and CA to release the peptides to the hemolymph. In addition, this result indicates the effectiveness of dsRNA, not just at mRNA but also peptide level, at least in the case of BgILP5.

With regard to *BgILP* expression in the brain throughout the gonadotrophic cycle, *BgILP3* and *BgILP5* show the greatest variations, with expression profiles paralleling that of JH synthesis (Maestro et al., 1994). The *BgILP1*, *2*, *4* and *6* expression profiles show lesser variations. Fat body *BgILP7* expression shows a profile approximately parallel to *Vg* expression (Martín et al., 1998), whereas ovarian *BgILP2* expression decreases during ovary maturation. Also, in *S. gregaria*, the expression of *IRP* in the fat body is higher in vitellogenic than in previtellogenic stages (Badisco et al., 2008). However, it should be taken into account that mRNA levels may not reflect peptide content and, even less so, the amount of peptide released to the hemolymph, which could be regulated by a different process to the expression. In fact, specific regulation of the release of ILPs synthesized in the brain has been demonstrated in *D. melanogaster* (Park et al., 2014).

The expression of *BgILP3*, *5* and *6* in the brain, and *BgILP7* in the fat body, is reduced in starved females. Also, in *D. melanogaster,* starvation reduces larval brain *dilp3* and *dilp5* expression and dilp2 release (Ikeya et al., 2002). Thus, in both species, some of the ILPs seem to be responsible for transducing nutritional signals. In the ovary, by contrast, *BgILP2* expression is increased in starved females. One possible explanation for this result is that ovaries from starved females remain in a physiologically and anatomically previtellogenic condition, and we have shown that previtellogenic ovaries have higher *BgILP2* mRNA levels than vitellogenic ones.

Although the RNAi treatment of each single BgILP induced an important depletion in the mRNA levels of the targeted BgILP, we recorded no reduced expression of either the enzymes analyzed for JH biosynthesis or *Vg*. However, the results did show increased *BgILP3* mRNA levels in dsILP5-treated females and a possible increase in *BgILP5* mRNA levels in ds-ILP3 treated females; this indicates some kind of compensatory effect at the transcriptional level between the two peptides. Comparable results have been reported for *D. melanogaster*, for example, *dilp2* mutants show greater *dilp3* and *dilp5* expression (Broughton et al., 2008; Grönke et al., 2010; Liu et al., 2016). In some cases the effect is produced even among different tissues, as *dilp6* overexpression in the fat body reduces brain *dilp2* and *dilp5* expression (Bai et al., 2012). In some other cases, a synergistic effect has been reported, as *dilp3* mutants show reduced *dilp2* and *dilp5* expression (Grönke et al., 2010).

Neither the knockdown of the three BgILPs that reduce their expression in starved insects (BgILP3, 5 and 6) nor the knockdown of all seven BgILPs produced the same phenotypes in terms of expression of JH biosynthesis enzymes, *Vg,* or ovary development, that we achieved by depleting InR. With regard to other insects, in the beetle *Leptinotarsa decemlineata*, RNAi-triggered depletion of ILP2, one of its five ILPs, produces a reduction in *JHAMT* mRNA and JH titer (Fu et al., 2016). Also in the coleopteran *Tribolium castaneum*, ILP depletion reduces *Vg* mRNA levels (Sheng et al., 2011). In *S. gregaria*, depletion of the only IRP induces a slight reduction of the *Vg1*, but not *Vg2*, mRNAs (Badisco et al., 2011). In *D. melanogaster*, the genetic ablation of IPCs or *dilp1* mutation reduces the number of eggs laid (Ikeya et al., 2002; Liu et al., 2016), whereas in the mosquito, *A. aegypti*, *ilp7* and *ilp8* mutations impair ovarian development (Ling et al., 2017).

The question remains as to why we were unable to achieve the same phenotypes by depleting all seven BgILPs as depleting InR. There are several possibilities. It is possible that there were further BgILPs that we did not detect in our analysis of the transcriptomes and genome, although we consider this improbable because the search was systematic and exhaustive. Interestingly, the recently published genome sequence of the American cockroach, *Periplaneta americana* (Li et al., 2018), revealed the occurrence of 7 ILP genes, despite it being larger (3.38 Gb) than that of *B. germanica* (2.5 Gb) (Harrison et al., 2018).

Another explanation involves the fact that the knockdown induced by RNAi does not completely eliminate the expression, and that the remaining ILPs, considering some possible redundancies in their effects, could be enough to facilitate the required functions. Nevertheless, at least in the case of BgILP5, we were unable to detect the peptide in our immunohistochemical analysis in the IPCs from dsILP5-treated animals. A further possible explanation could be that, although in different insect species it has been demonstrated that InR binds ILPs and that InR occurrence is necessary for ILP activity (Brown et al., 2008; Roy et al., 2007; Rulifson et al., 2002), InR has a function that is independent of ILPs. Finally, we cannot rule out the possibility of greater availability of InR in the cell membranes of dsILP1-7 animals, considering the proposed recycling of membrane receptors in general and that of InR in particular (Knutson, 1991).

In conclusion, we have identified seven ILPs in the cockroach *B. germanica* and have demonstrated that they are differentially expressed in tissues, during the gonadotrophic cycle and in response to starvation. In addition, by knocking down the BgILPs we were able to identify compensatory regulation at the transcriptional level between different BgILPs. The next challenges include defining the role of BgILPs in certain other functions regulated by the IIS pathway, such as, for example, growth. It would also be interesting to determine the functions of the two other InR genes recently described in cockroaches (Kremer et al., 2018) and their respective relationships with BgILPs.

Acknowledgements

This work was supported by grants BFU2010-15906 (Spanish Ministry of Science and Innovation (MICINN)), CGL2016-76011-R (Spanish Ministry of Economy and Competitiveness (MINECO) and FEDER) and 2014-SGR-619 (*Secretaria d'Universitats i Recerca*, Catalan Goverment) to J.L.M. Thanks are due to the Human Genome Sequencing Center at the Baylor College of Medicine for the access to the German Cockroach Genome Project. Thanks to Xavier Bellés for critical reading of the manuscript.

References

Abrisqueta, M., Süren-Castillo, S., Maestro, J.L., 2017. S6 protein kinase activates Juvenile Hormone and vitellogenin production in the cockroach Blattella germanica. Physiol. Entomol. 42. doi:10.1111/phen.12156

Abrisqueta, M., Süren-Castillo, S., Maestro, J.L., 2014. Insulin receptor-mediated nutritional signalling regulates juvenile hormone biosynthesis and vitellogenin production in the German cockroach. Insect Biochem. Mol. Biol. 49, 14–23. doi:10.1016/j.ibmb.2014.03.005

Antonova, Y., Arik, A.J., Moore, W., Riehle, M.A., Brown, M.R., 2012. Insulin-Like Peptides: Structure, Signaling, and Function, in: Gilbert, L.I. (Ed.), Insect Endocrinology. Elsevier, pp. 63–92. doi:10.1016/B978-0-12-384749-2.10002-0

Aslam, A.F.M., Kiya, T., Mita, K., Iwami, M., 2011. Identification of Novel Bombyxin Genes from the Genome of the Silkmoth *Bombyx mori* and Analysis of their Expression. Zoolog. Sci. 28, 609–616. doi:10.2108/zsj.28.609

Badisco, L., Claeys, I., Van Hiel, M., Clynen, E., Huybrechts, J., Vandersmissen, T., Van Soest, S., Vanden Bosch, L., Simonet, G., Vanden Broeck, J., 2008. Purification and characterization of an insulin-related peptide in the desert locust, Schistocerca gregaria: immunolocalization, cDNA cloning, transcript profiling and interaction with neuroparsin. J. Mol. Endocrinol. 40, 137–50. doi:10.1677/JME-07-0161

Badisco, L., Marchal, E., Van Wielendaele, P., Verlinden, H., Vleugels, R., Vanden Broeck, J., 2011. RNA interference of insulin-related peptide and neuroparsins affects vitellogenesis in the desert locust Schistocerca gregaria. Peptides 32, 573–80. doi:10.1016/j.peptides.2010.11.008

Bai, H., Kang, P., Tatar, M., 2012. Suppl. Results. Drosophila insulin-like peptide-6 (dilp6) expression from fat body extends lifespan and represses secretion of Drosophila insulin-like peptide-2 from the brain. Aging Cell 11, 978–85. doi:10.1111/acel.12000

Bermudez, I., Beadle, D.J., Trifilieff, E., Luu, B., Hietter, H., 1991. Electrophysiological activity of the C-peptide of the *Locusta* insulin-related peptide Effect on the membrane conductance of *Locusta* neurones in vitro. FEBS Lett. 293, 137–141. doi:10.1016/0014-5793(91)81170-D

Brogiolo, W., Stocker, H., Ikeya, T., Rintelen, F., Fernandez, R., Hafen, E., 2001. An evolutionarily conserved function of the Drosophila insulin receptor and insulin-like peptides in growth control. Curr. Biol. 11, 213–221.

Broughton, S., Alic, N., Slack, C., Bass, T., Ikeya, T., Vinti, G., Tommasi, A.M., Driege, Y., Hafen, E., Partridge, L., 2008. Reduction of DILP2 in Drosophila triages a metabolic phenotype from lifespan revealing redundancy and compensation among DILPs. PLoS One 3, e3721. doi:10.1371/journal.pone.0003721

Broughton, S.J., Piper, M.D.W., Ikeya, T., Bass, T.M., Jacobson, J., Driege, Y., Martinez, P., Hafen, E., Withers, D.J., Leevers, S.J., Partridge, L., Kenyon, C.J., 2005. Longer lifespan, altered metabolism, and stress resistance in Drosophila from ablation of cells making insulin-like ligands. Proc. Natl. Acad. Sci. 102, 3105–3110.

Brown, M.R., Clark, K.D., Gulia, M., Zhao, Z., Garczynski, S.F., Crim, J.W., Suderman, R.J., Strand, M.R., 2008. An insulin-like peptide regulates egg maturation and metabolism in the mosquito Aedes aegypti. Proc. Natl. Acad. Sci. U. S. A. 105, 5716–21. doi:10.1073/pnas.0800478105

Claeys, I., Simonet, G., Poels, J., Van Loy, T., Vercammen, L., De Loof, A., Vanden Broeck, J., 2002. Insulin-related peptides and their conserved signal transduction pathway. Peptides 23, 807–816. doi:10.1016/S0196-9781(01)00666-0

Clynen, E., Huybrechts, J., Baggerman, G., Van Doorn, J., Van Der Horst, D., De Loof, A., Schoofs, L., 2003. Identification of a glycogenolysis-inhibiting peptide from the corpora cardiaca of locusts. Endocrinology 144, 3441–8. doi:10.1210/en.2002-0107

Colombani, J., Andersen, D.S., Boulan, L., Virolle, V., Texada, M., Lé, P., 2015. Drosophila Lgr3 Couples Organ Growth with Maturation and Ensures Developmental Stability In Brief. Curr. Biol. 25, 2723–2729. doi:10.1016/j.cub.2015.09.020

Dominguez, C. V., Maestro, J.L., 2018. Expression of juvenile hormone acid O - methyltransferase and juvenile hormone synthesis in Blattella germanica. Insect Sci. 25, 787–796. doi:10.1111/1744-7917.12467

Fu, K.-Y., Zhu, T.-T., Guo, W.-C., Ahmat, T., Li, G.-Q., 2016. Knockdown of a putative insulin-like peptide gene LdILP2 in Leptinotarsa decemlineata by RNA interference impairs pupation and adult emergence. Gene 581, 170–7. doi:10.1016/j.gene.2016.01.037

Garelli, A., Heredia, F., Casimiro, A.P., Macedo, A., Nunes, C., Garcez, M., Dias, A.R.M., Volonte, Y.A., Uhlmann, T., Caparros, E., Koyama, T., Gontijo, A.M., 2015. Dilp8 requires the neuronal relaxin receptor Lgr3 to couple growth to developmental timing. Nat. Commun. 6, 8732. doi:10.1038/ncomms9732

Géminard, C., Rulifson, E.J., Léopold, P., 2009. Remote control of insulin secretion by fat cells in Drosophila. Cell Metab. 10, 199–207. doi:10.1016/j.cmet.2009.08.002

Grönke, S., Clarke, D.-F., Broughton, S., Andrews, T.D., Partridge, L., 2010. Molecular evolution and functional characterization of Drosophila insulin-like peptides. PLoS Genet. 6, e1000857. doi:10.1371/journal.pgen.1000857

Gulia-Nuss, M., Robertson, A.E., Brown, M.R., Strand, M.R., 2011. Insulin-Like Peptides and the Target of Rapamycin Pathway Coordinately Regulate Blood Digestion and Egg Maturation in the Mosquito Aedes aegypti. PLoS One 6, e20401. doi:10.1371/journal.pone.0020401

Harrison, M.C., Jongepier, E., Robertson, H.M., Arning, N., Bitard-Feildel, T., Chao, H., Childers, C.P., Dinh, H., Doddapaneni, H., Dugan, S., Gowin, J., Greiner, C., Han, Y., Hu, H., Hughes, D.S.T., Huylmans, A.-K., Kemena, C., Kremer, L.P.M., Lee, S.L., Lopez-Ezquerra, A., Mallet, L., Monroy-Kuhn, J.M., Moser, A., Murali, S.C., Muzny, D.M., Otani, S., Piulachs, M.-D., Poelchau, M., Qu, J., Schaub, F., Wada-Katsumata, A., Worley, K.C., Xie, Q., Ylla, G., Poulsen, M., Gibbs, R.A., Schal, C., Richards, S., Belles, X., Korb, J., Bornberg-Bauer, E., 2018. Hemimetabolous genomes reveal molecular basis of termite eusociality. Nat. Ecol. Evol. 2, 557–566. doi:10.1038/s41559-017-0459-1

Humbel, R.E., 1990. Insulin-like growth factors I and II. Eur. J. Biochem. 190, 445–462.

doi:10.1111/j.1432-1033.1990.tb15595.x

Ikeya, T., Galic, M., Belawat, P., Nairz, K., Hafen, E., 2002. Nutrient-dependent expression of insulin-like peptides from neuroendocrine cells in the CNS contributes to growth regulation in Drosophila. Curr. Biol. 12, 1293–1300. doi:10.1016/S0960-9822(02)01043-6

Irles, P., Piulachs, M.-D., 2014. Unlike in Drosophila Meroistic Ovaries, Hippo Represses Notch in Blattella germanica Panoistic Ovaries, Triggering the Mitosis-Endocycle Switch in the Follicular Cells. PLoS One 9, e113850. doi:10.1371/journal.pone.0113850

Knutson, V.P., 1991. Cellular trafficking and processing of the insulin receptor. FASEB J. 5, 2130–8.

Krieger, M.J.B., Jahan, N., Riehle, M.A., Cao, C., Brown, M.R., 2004. Molecular characterization of insulin-like peptide genes and their expression in the African malaria mosquito, Anopheles gambiae. Insect Mol. Biol. 13, 305–15. doi:10.1111/j.0962-1075.2004.00489.x

Lagueux, M., Lwoff, L., Meister, M., Goltzene, F., Hoffmann, J.A., 1990. cDNAs from neurosecretory cells of brains of Locusta migratoria (Insecta, Orthoptera) encoding a novel member of the superfamily of insulins. Eur. J. Biochem. 187, 249–254. doi:10.1111/j.1432-1033.1990.tb15302.x

Li, S., Zhu, S., Jia, Q., Yuan, D., Ren, C., Li, K., Liu, S., Cui, Y., Zhao, H., Cao, Y., Fang, G., Li, D., Zhao, X., Zhang, J., Yue, Q., Fan, Y., Yu, X., Feng, Q., Zhan, S., 2018. The genomic and functional landscapes of developmental plasticity in the American cockroach. Nat. Commun. 9, 1008. doi:10.1038/s41467-018-03281-1

Ling, L., Kokoza, V.A., Zhang, C., Aksoy, E., Raikhel, A.S., 2017. MicroRNA-277 targets insulin-like peptides 7and 8 to control lipid metabolism and reproduction in Aedes aegypti mosquitoes. Proc. Natl. Acad. Sci. U. S. A. 114, E8017–E8024. doi:10.1073/pnas.1710970114

Liu, Y., Liao, S., Veenstra, J.A., Nässel, D.R., 2016. Drosophila insulin-like peptide 1 (DILP1) is transiently expressed during non-feeding stages and reproductive dormancy. Sci. Rep. 6, 26620. doi:10.1038/srep26620

Lu, K., Chen, X., Li, W., Li, Y., Zhang, Z., Zhou, Q., 2018. Insulin-like peptides and DNA/tRNA methyltransferases are involved in the nutritional regulation of female reproduction in Nilaparvata lugens (Stål). Gene 639, 96–105. doi:10.1016/J.GENE.2017.10.011

Maestro, J.L., Cobo, J., Bellés, X., 2009. Target of rapamycin (TOR) mediates the transduction of nutritional signals into juvenile hormone production. J. Biol. Chem. 284, 5506–5513.

Maestro, J.L., Danés, M.D., Piulachs, M.D., Cassier, P., Bellés, X., 1994. Juvenile Hormone inhibition in corpora allata from ovariectomized Blattella germanica. Physiol. Entomol. 19, 342–348. doi:10.1111/j.1365-3032.1994.tb01061.x

Martín, D., Piulachs, M.-D., Comas, D., Bellés, X., 1998. Isolation and sequence of a partial

vitellogenin cDNA from the cockroach,Blattella germanica (L.) (Dictyoptera, Blattellidae), and characterization of the vitellogenin gene expression. Arch. Insect Biochem. Physiol. 38, 137–146. doi:10.1002/(SICI)1520-6327(1998)38:3<137::AID-ARCH4>3.0.CO;2-P

Nagasawa, H., Kataoka, H., Isogai, A., Tamura, S., Suzuki, A., Ishizaki, H., Mizoguchi, A., Fujiwara, Y., Suzuki, A., 1984. Amino-terminal amino Acid sequence of the silkworm prothoracicotropic hormone: homology with insulin. Science 226, 1344–5. doi:10.1126/science.226.4680.1344

Okamoto, N., Yamanaka, N., Satake, H., Saegusa, H., Kataoka, H., Mizoguchi, A., 2009a. An ecdysteroid-inducible insulin-like growth factor-like peptide regulates adult development of the silkmoth Bombyx mori. FEBS J. 276, 1221–1232. doi:10.1111/j.1742-4658.2008.06859.x

Okamoto, N., Yamanaka, N., Yagi, Y., Nishida, Y., Kataoka, H., O'Connor, M.B., Mizoguchi, A., 2009b. A fat body-derived IGF-like peptide regulates postfeeding growth in Drosophila. Dev. Cell 17, 885–91. doi:10.1016/j.devcel.2009.10.008

Ons, S., Bellés, X., Maestro, J.L., 2015. Orcokinins contribute to the regulation of vitellogenin transcription in the cockroach Blattella germanica. J. Insect Physiol. 82, 129–33. doi:10.1016/j.jinsphys.2015.10.002

Park, S., Alfa, R.W., Topper, S.M., Kim, G.E.S., Kockel, L., Kim, S.K., 2014. A genetic strategy to measure circulating Drosophila insulin reveals genes regulating insulin production and secretion. PLoS Genet. 10, e1004555. doi:10.1371/journal.pgen.1004555

Patil, N.A., Rosengren, K.J., Separovic, F., Wade, J.D., Bathgate, R.A.D., Hossain, M.A., 2017. Relaxin family peptides: structure-activity relationship studies. Br. J. Pharmacol. 174, 950–961. doi:10.1111/bph.13684

Perez-Hedo, M., Rivera-Perez, C., Noriega, F.G., 2014. Starvation increases insulin sensitivity and reduces juvenile hormone synthesis in mosquitoes. PLoS One 9, e86183. doi:10.1371/journal.pone.0086183

Pérez-Hedo, M., Rivera-Perez, C., Noriega, F.G., 2013. The insulin/TOR signal transduction pathway is involved in the nutritional regulation of juvenile hormone synthesis in Aedes aegypti. Insect Biochem. Mol. Biol. 43, 495–500. doi:10.1016/j.ibmb.2013.03.008

Petersen, T.N., Brunak, S., von Heijne, G., Nielsen, H., 2011. SignalP 4.0: discriminating signal peptides from transmembrane regions. Nat. Methods 8, 785–786. doi:10.1038/nmeth.1701

Riehle, M.A., Fan, Y., Cao, C., Brown, M.R., 2006. Molecular characterization of insulin-like peptides in the yellow fever mosquito, Aedes aegypti: expression, cellular localization, and phylogeny. Peptides 27, 2547–60. doi:10.1016/j.peptides.2006.07.016

Roy, S.G., Hansen, I.A., Raikhel, A.S., 2007. Effect of insulin and 20-hydroxyecdysone in the fat body of the yellow fever mosquito, Aedes aegypti. Insect Biochem. Mol. Biol. 37, 1317–26. doi:10.1016/j.ibmb.2007.08.004

Rulifson, E.J., Kim, S.K., Nusse, R., 2002. Ablation of insulin-producing neurons in flies: growth and diabetic phenotypes. Science 296, 1118–20. doi:10.1126/science.1070058

Sheng, Z., Xu, J., Bai, H., Zhu, F., Palli, S.R., 2011. Juvenile hormone regulates vitellogenin gene expression through insulin-like peptide signaling pathway in the red flour beetle, Tribolium castaneum. J. Biol. Chem. 286, 41924–41936. doi:10.1074/jbc.M111.269845

Slaidina, M., Delanoue, R., Gronke, S., Partridge, L., Léopold, P., 2009. A Drosophila insulin-like peptide promotes growth during nonfeeding states. Dev. Cell 17, 874–84. doi:10.1016/j.devcel.2009.10.009

Süren-Castillo, S., Abrisqueta, M., Maestro, J.L., 2012. FoxO inhibits juvenile hormone biosynthesis and vitellogenin production in the German cockroach. Insect Biochem. Mol. Biol. 42, 491–498.

Tatar, M., Kopelman, A., Epstein, D., Tu, M.P., Yin, C.M., Garofalo, R.S., 2001. A mutant Drosophila insulin receptor homolog that extends life-span and impairs neuroendocrine function. Science 292, 107–10. doi:10.1126/science.1057987

Vallejo, D.M., Juarez-Carreño, S., Bolivar, J., Morante, J., Dominguez, M., 2015. A brain circuit that synchronizes growth and maturation revealed through Dilp8 binding to Lgr3. Science (80-.). 350, aac6767. doi:10.1126/science.aac6767

Van de Velde, S., Badisco, L., Claeys, I., Verleyen, P., Chen, X., Vanden Bosch, L., Vanden Broeck, J., Smagghe, G., 2007. Insulin-like peptides in Spodoptera littoralis (Lepidoptera): Detection, localization and identification. Gen. Comp. Endocrinol. 153, 72–9. doi:10.1016/j.ygcen.2007.05.001

Veenstra, J.A., 2000. Mono- and dibasic proteolytic cleavage sites in insect neuroendocrine peptide precursors. Arch. Insect Biochem. Physiol. 43, 49–63. doi:10.1002/(SICI)1520-6327(200002)43:2<49::AID-ARCH1>3.0.CO;2-M

Veenstra, J.A., Agricola, H.-J., Sellami, A., 2008. Regulatory peptides in fruit fly midgut. Cell Tissue Res. 334, 499–516. doi:10.1007/s00441-008-0708-3

Wu, Q., Brown, M.R., 2006. Signaling and function of Insulin-like Peptides in insects. Annu. Rev. Entomol. 51, 1–24. doi:10.1146/annurev.ento.51.110104.151011

Ylla, G., Piulachs, M.-D., Belles, X., 2018. Comparative Transcriptomics in Two Extreme Neopterans Reveals General Trends in the Evolution of Modern Insects. iScience 4, 164–179. doi:10.1016/J.ISCI.2018.05.017

Figure legends

Figure 1. *Blattella germanica* ILP sequences. Amino acid sequences of *B. germanica* insulin-like peptides 1 to 7 (BgILP1-7). The signal peptide for each ILP is underlined. B-

chains, C-peptides, and A-chains are highlighted in blue, yellow, and pink, respectively. The characteristic cysteines of insulin-like sequences are in red. The single or pair basic amino acids that provide the cleavage sites for producing the final mature protein are in green.

Figure 2. *BgILP* expression in *B. germanica* tissues. *BgILP* mRNA levels were quantified in different tissues of 5-day-old adult females. CC = corpora cardiaca, CA = corpora allata, FB = fat body. Y-axes indicate copies per copy of *Actin 5C*. The results are expressed as the mean ± S.E. (n = 3).

Figure 3. Immunolocalization of BgILP5 in the brains of control and dsILP5-treated adult *B. germanica* females. Adult *B. germanica* females were treated with dsRNA targeting BgILP5 (dsILP5) or a heterologous dsRNA (Control) during the oothecal transport period, and dissections and immunohistochemistry were performed on day 5 of the second gonadotrophic cycle (see Material and Methods). (A) Immunostained brain from a control female showing labeled insulin-producing cells (IPCs) in the pars intercerebralis. (B) The immunostained brain from a dsILP5-treated female shows no labeling in any IPC (arrow). The images are representative of at least 3 brains per treatment. BgILP5, pink; DAPI, blue. Scale bars: 100 µm.

Figure 4. Brain *BgILP* expression throughout the *B. germanica* gonadotrophic cycle. Expression patterns of *BgILP1-6* in female brains on selected days in the first gonadotrophic cycle. Y-axes indicate copies per copy of *Actin 5C*. The results are expressed as the mean ± S.E. (n = 3). The different letters (a-b) indicate groups with significant differences according to the ANOVA test (Tukey, $p < 0.05$).

Figure 5. *BgILP* expression in fed and starved *B. germanica* females. Samples were obtained from 5-day-old adult females. (A) *BgILP1-6* mRNA levels in brains (n = 4-5). (B) *BgILP7* mRNA levels in fat bodies (n = 4). (C) *BgILP2* mRNA levels in ovaries (n = 5). Y-axes indicate copies per copy of *Actin 5C*. The results are expressed as the mean ± S.E. An asterisk represents significant differences between fed and starved subjects (Student's t-test, $*p < 0.05$; $**p < 0.001$; $***p < 0.0001$).

Figure 6. Effect of BgILP3 RNAi on *BgILP* expression. Adult *B. germanica* females were treated with dsRNA targeting BgILP3 (dsILP3) or a heterologous dsRNA (Control) during the oothecal transport period, and dissections were performed on day 5 of the second gonadotrophic cycle (see Material and Methods). (A) *BgILP1-6* mRNA levels in brains (n = 5-7). (B) *BgILP7* mRNA levels in fat bodies (n = 4-7). Y-axes indicate copies per copy of *Actin 5C*. The results are expressed as the mean ± S.E. An asterisk represents significant differences between control and dsILP3 subjects (Student's t-test, $***p < 0.0001$).

Figure 7. Effect of BgILP5 RNAi on *BgILP* expression and ovarian growth. Adult *B. germanica* females were treated with dsRNA targeting BgILP5 (dsILP5) or a heterologous

dsRNA (Control) during the oothecal transport period, and dissections were performed on day 5 of the second gonadotrophic cycle (see Material and Methods). (A) *BgILP1-6* mRNA levels in brains (n = 12). (B) *BgILP7* mRNA levels in fat bodies (n = 9-10). (C) Basal follicle length (n = 22-25). In A and B, the Y-axes indicate copies per copy of *Actin 5C*. The results are expressed as the mean ± S.E. An asterisk represents significant differences between control and dsILP5 subjects (Student's t-test, $^{**}p < 0.005$; $^{***}p < 0.0001$).

Figure 8. Effect of the knockdown of the seven BgILPs on the expression of *BgILPs*, JH biosynthesis enzymes and *Vg*, and ovarian growth. Adult *B. germanica* females were treated with dsRNA targeting all seven BgILPs (dsILP1-7) or a heterologous dsRNA (Control) during the oothecal transport period, and dissections were performed on day 5 of the second gonadotrophic cycle (see Material and Methods). (A) *BgILP1-6* mRNA levels in brains (n = 7-8). (B) *HMG-CoA synthase-1* (*HMG-S1*), *HMG-CoA reductase* (*HMG-R*), *JHAMT* and *InR* mRNA levels in CC-CA (n = 7). (C) *BgILP7* and *Vg* mRNA levels in fat bodies (n = 6-7). (D) Basal follicle length (n = 8). In A, B and C, the Y-axes indicate copies per copy of *Actin 5C*. The results are expressed as the mean ± S.E. An asterisk represents significant differences between control and dsILP1-7 subjects (Student's t-test, $^{*}p < 0.05$; $^{**}p < 0.01$; $^{***}p < 0.0001$).

BgILP1:MVWKFCLCVMIVSIMCACALPENPSTMFQFVRKRETPHRYCGRHLVSILQLLCGSNYNGDIEKKRSSEIRD
SKPMQDADELPWLQSQPFEEGSEAEFPFRSRSVANSLRNRLFRRHSRDGGIVDECCIYKGCTTSELAEYCLDR

BgILP2:MWRICLQLVAIAALCLCTLAQAQSDLFQFADKRNTNKYCGRNLANMLQLVCNGNYYPMFKKSSQDMDDMN
DSGFWIQPSTMEEQQLQYPFRSRSSASALVSGSFRRRTRGVYDECCRKSCSIQEMASYCGKR

BgILP3:MWKVFLKLVVLMTICFSLSESQSDLIEFMEKRQSKRYCGNKLVDMVRLVCSSVYYTPSPKSTTTTTTTQIP
SLDKKSDDAGDDFWMQRLIQESEDQYYMFPFQSEARAHNILKRYPRGIANECCIYKGCTIEELMSYCGK

BgILP4:MWQAFCRLLIIVTVCVSLSESQSDVYQMMDKRQTRRYCGSNLVEIMQFVCNGSYNGMSTHLSQKKSETDDD
FWMQLLQGEEQYKYPFRSRSSAHRIFKRYPGGIAYECCISKGCNIYELRSYCAPSSK

BgILP5:MKMWKILLAIAIVGIVWSNALPKDSASKMHMIRKRQSTHRYCGPHLVSALRLLCNGRYYTPDEDEDDTTTE
KRSTTTNELEDIDNPILAKRKYSEESEKPQFPFRSREEANSLKPKFFRRKRRMIVEECCNLKGCSVNELMEYCAD

BgILP6:MKNAYLSLFLAAVTCFCLSDCQSETFQVDKRHASRKYCGHNLVLVMQLVCDSRYNSPRPSNPSKKSDTDDF
WQQLEVQSSEQEYRFPFRSLSNAFRLMKRGGGIADECCYNKGCTYVELRSYCST

BgILP7:MLKCGIVTALVLVTTMVSGAPTIRMQMCGSQLANTLAQICSAYGYHDPFSQTRRVNSPSSGVNTTPNRLRVRR
GVADECCKTGCTLDTMEQYCSAPLTPAQR

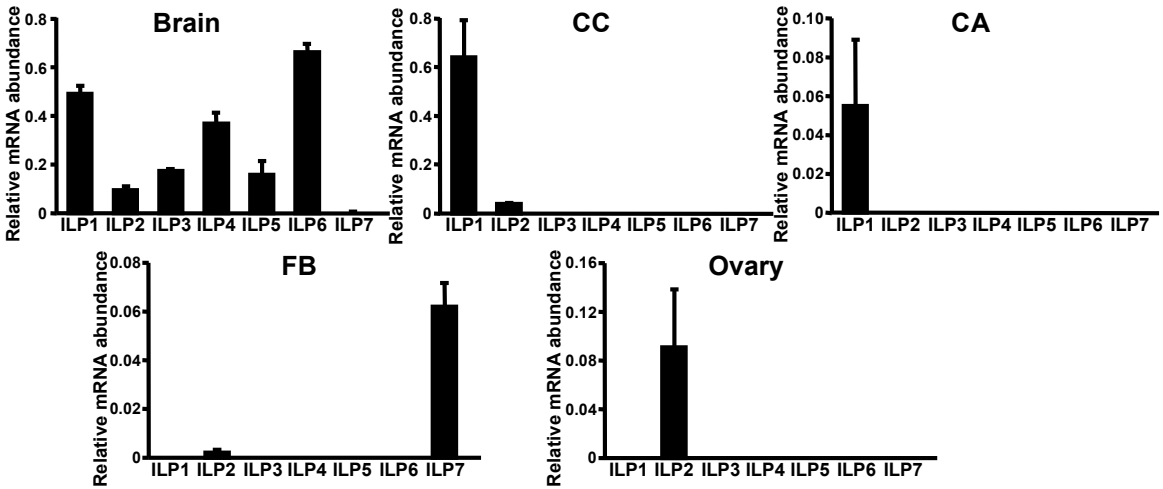
Brain
CC
CA
FB
Ovary
Relative mRNA abundance
ILP1 ILP2 ILP3 ILP4 ILP5 ILP6 ILP7
0
0.2
0.4
0.6
0.8
0.02
0.04
0.06
0.08
0.10
0.12
0.16

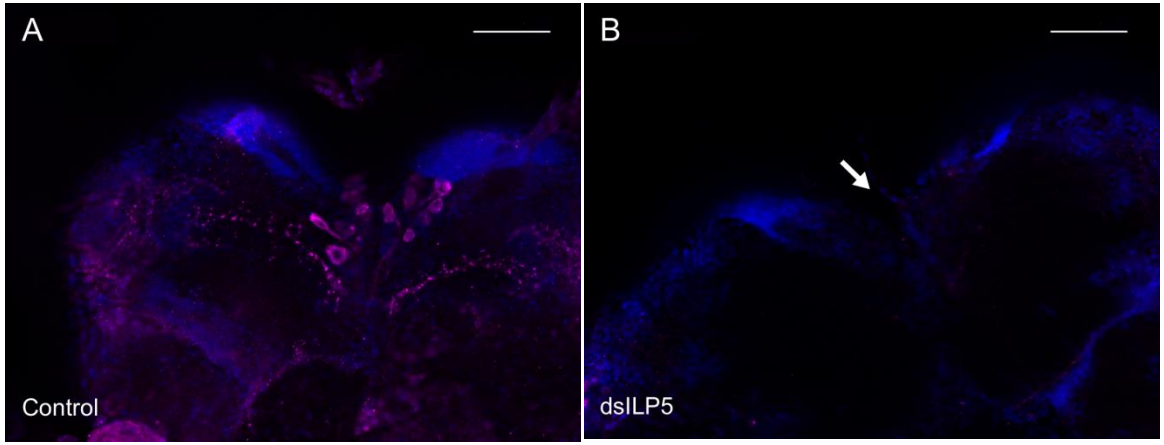
A
Control
B
dsILP5

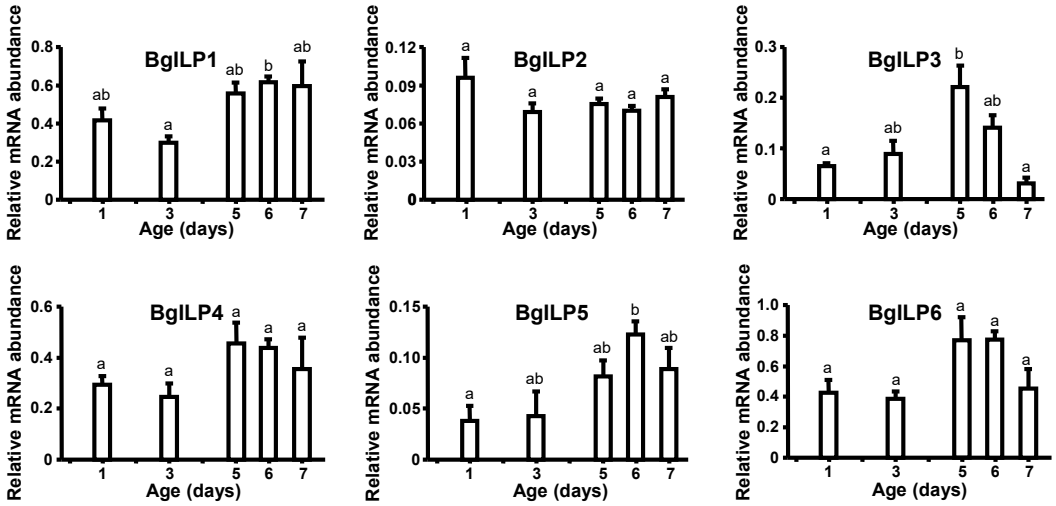
BgILP1
Relative mRNA abundance
0.8
0.6
0.4
0.2
0
ab
a
ab
b
ab
1
3
5
6
7
Age (days)
BgILP2
Relative mRNA abundance
0.12
0.09
0.06
0.03
0
a
a
a
a
a
1
3
5
6
7
Age (days)
BgILP3
Relative mRNA abundance
0.3
0.2
0.1
0
a
ab
b
ab
a
1
3
5
6
7
Age (days)
BgILP4
Relative mRNA abundance
0.6
0.4
0.2
0
a
a
a
a
a
1
3
5
6
7
Age (days)
BgILP5
Relative mRNA abundance
0.15
0.10
0.05
0
a
ab
ab
b
ab
1
3
5
6
7
Age (days)
BgILP6
Relative mRNA abundance
1.0
0.8
0.6
0.4
0.2
0
a
a
a
a
a
1
3
5
6
7
Age (days)

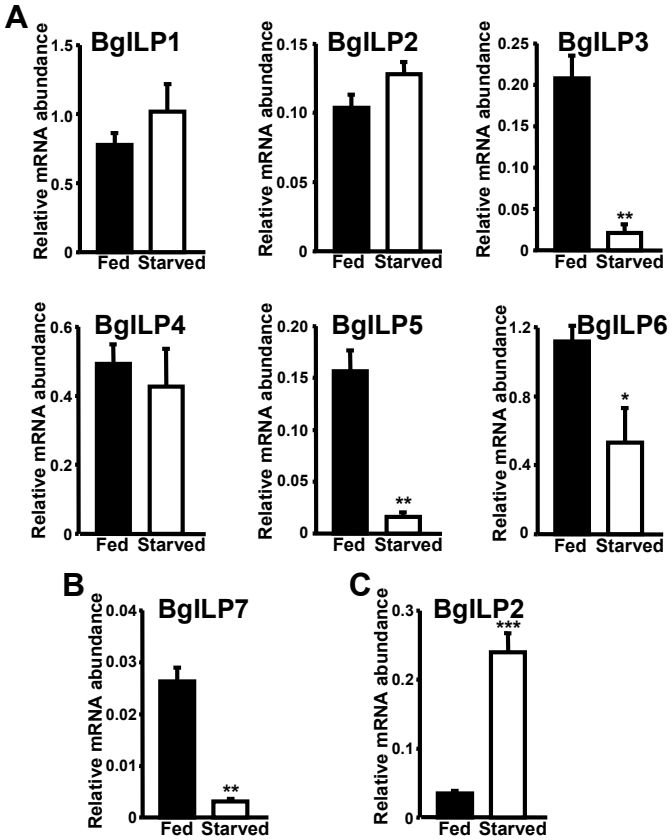
A
BglLP1
BglLP2
BglLP3
BglLP4
BglLP5
BglLP6
Relative mRNA abundance
Fed
Starved
**
*
B
BglLP7
C
BglLP2
***

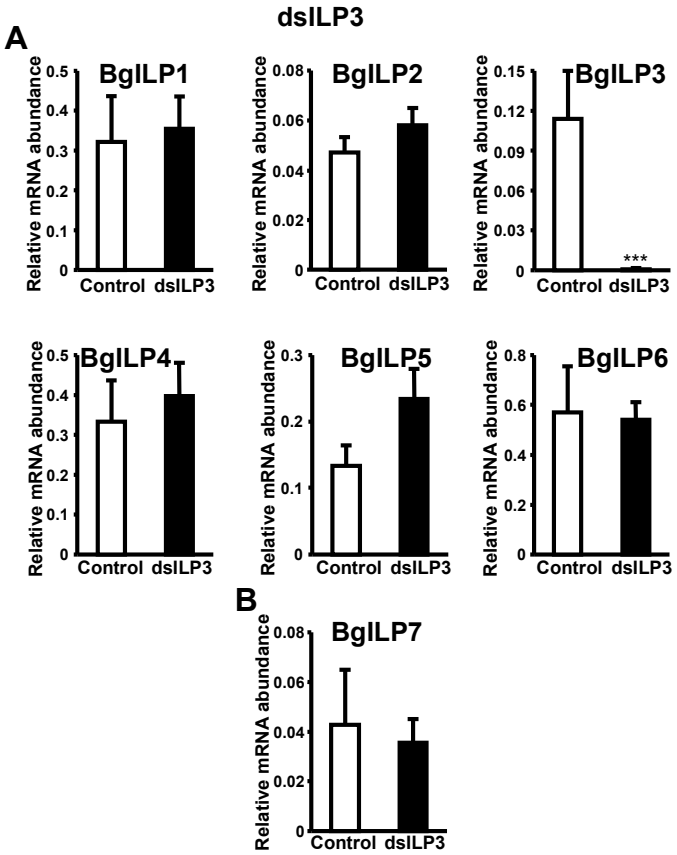
dsILP3
A
BgILP1
BgILP2
BgILP3
BgILP4
BgILP5
BgILP6
B
BgILP7
Relative mRNA abundance
Control
dsILP3
***

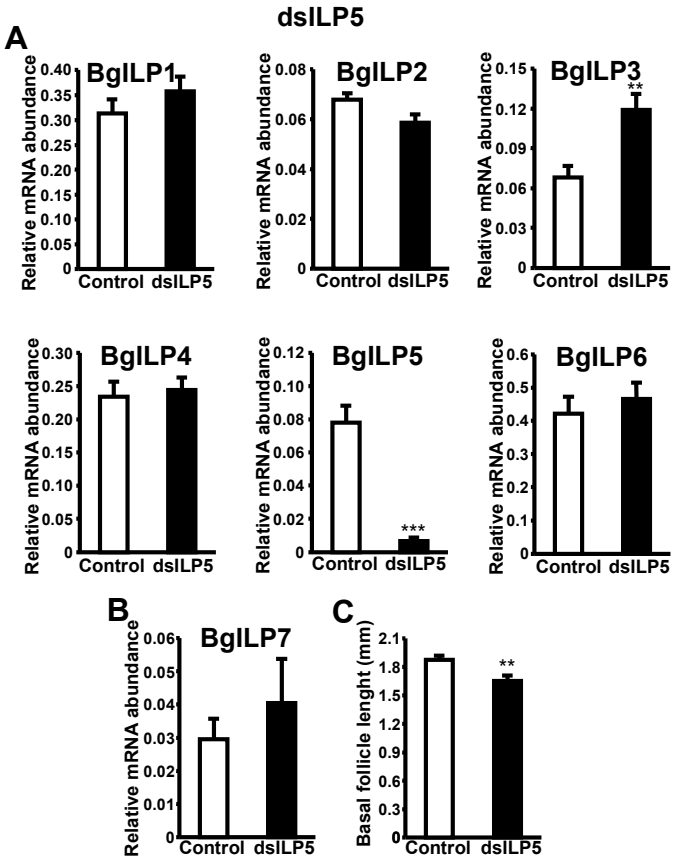
dsILP5
A
BgILP1
BgILP2
BgILP3
BgILP4
BgILP5
BgILP6
Relative mRNA abundance
Control
dsILP5
**
***
B
BgILP7
C
Basal follicle lenght (mm)

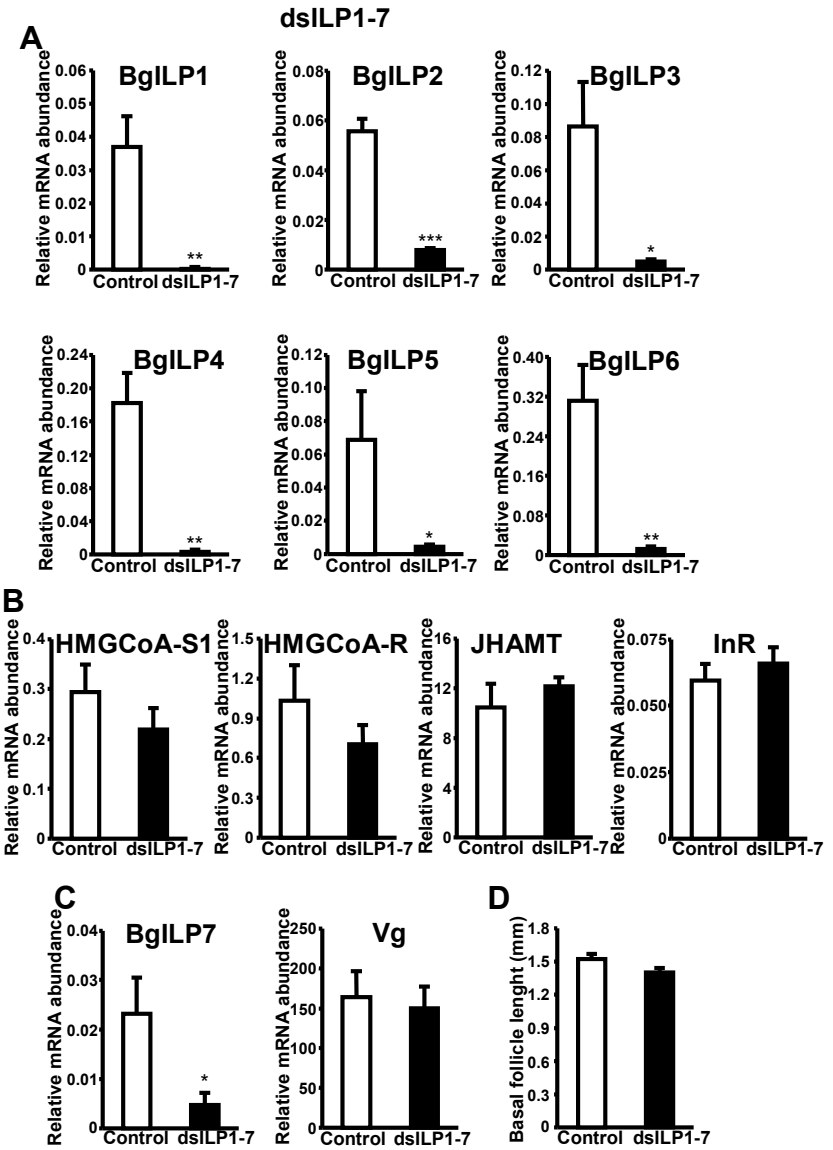
dsILP1-7
A
BgILP1
BgILP2
BgILP3
BgILP4
BgILP5
BgILP6
Relative mRNA abundance
Control
dsILP1-7
B
HMGCoA-S1
HMGCoA-R
JHAMT
InR
C
BgILP7
Vg
D
Basal follicle lenght (mm)

Supplementary figure legends

Figure S1. Fat body and ovary *BgILP* expression throughout the *B. germanica* gonadotrophic cycle. Expression patterns of *BgILP7* and *BgILP2* in female fat bodies and ovaries, respectively, on selected days in the first gonadotrophic cycle. Y-axes indicate copies per copy of *Actin 5C*. The results are expressed as the mean ± S.E. (n = 3). The different letters (a-b) indicate groups with significant differences according to the ANOVA test (Tukey, $p < 0.05$).

Figure S2. Effect of BgILP1 RNAi on the expression of *BgILPs*, JH biosynthesis enzymes and *Vg*, and on ovarian growth. Adult *B. germanica* females were treated with dsRNA targeting BgILP1 (dsILP1) or a heterologous dsRNA (Control) during the oothecal transport period, and dissections were performed on day 5 of the second gonadotrophic cycle (see Material and Methods). (A) *BgILP1-6* mRNA levels in brains (n = 8). (B) *BgILP1*, *HMG-CoA synthase-1* (*HMG-S1*), *HMG-CoA reductase* (*HMG-R*) and *JHAMT* mRNA levels in CC-CA (n = 4-6). (C) *BgILP7* and *Vg* mRNA levels in fat bodies (n = 7-8). (D) Basal follicle length (n = 8). In A, B and C the Y-axes indicate copies per copy of *Actin 5C*. The results are expressed as the mean ± S.E. An asterisk represents significant differences between control and dsILP1 subjects (Student's t-test, $^{**}p < 0.0005$; $^{***}p < 0.0001$).

Figure S3. Effect of BgILP2 RNAi on the expression of *BgILPs*, JH biosynthesis enzymes and *Vg*, and on ovarian growth. Adult *B. germanica* females were treated with dsRNA targeting BgILP2 (dsILP2) or a heterologous dsRNA (Control) during the oothecal transport period and dissections were performed on day 5 of the second gonadotrophic cycle (see Material and Methods). (A) *BgILP1-6* mRNA levels in brains (n = 5-7). (B) *HMG-CoA synthase-1* (*HMG-S1*), *HMG-CoA reductase* (*HMG-R*) and *JHAMT* mRNA levels in CC-CA (n = 4-6). (C) *BgILP7* and *Vg* mRNA levels in fat bodies (n = 4-6). (D) *BgILP2* mRNA levels in ovaries (n = 5). (E) Basal follicle length (n = 5-7). In A, B, C and D the Y-axes indicate copies per copy of *Actin 5C*. The results are expressed as the mean ± S.E. An asterisk represents significant differences between control and dsILP2 subjects (Student's t-test, $^{**}p < 0.0005$; $^{***}p < 0.0001$).

Figure S4. Effect of BgILP3 RNAi on the expression of JH biosynthesis enzymes and *Vg*, and on ovarian growth. Adult *B. germanica* females were treated with dsRNA targeting BgILP3 (dsILP3) or a heterologous dsRNA (Control) during the oothecal transport period and dissections were performed on day 5 of the second gonadotrophic cycle (see Material and Methods). (A) *HMG-CoA synthase-1* (*HMG-S1*), *HMG-CoA reductase* (*HMG-R*) and *JHAMT* mRNA levels in CC-CA (n = 4-6). (B) *Vg* mRNA levels in fat bodies (n = 4-7). (C) Basal follicle length (n = 5-7). In A and B the Y-axes indicate copies per copy of *Actin 5C*. The results are expressed as the mean ± S.E. An asterisk represents significant differences between control and dsILP3 subjects (Student's t-test, $^{*}p < 0.05$).

Figure S5. Effect of BgILP4 RNAi on the expression of *BgILPs*, JH biosynthesis enzymes and *Vg*, and on ovarian growth. Adult *B. germanica* females were treated with dsRNA targeting BgILP4 (dsILP4) or a heterologous dsRNA (Control) during the oothecal transport period and dissections were performed on day 5 of the second gonadotrophic cycle (see Material and Methods). (A) *BgILP1-6* mRNA levels in brains (n = 7). (B) *HMG-CoA synthase-1* (*HMG-S1*), *HMG-CoA reductase* (*HMG-R*) and *JHAMT* mRNA levels in CC-CA (n = 4-6). (C) BgILP7 and *Vg* mRNA levels in fat bodies (n = 8-10). (D) Basal follicle length (n = 13-18). In A, B and C the Y-axes indicate copies per copy of *Actin 5C*. The results are expressed as the mean ± S.E. An asterisk represents significant differences between control and dsILP4 subjects (Student's t-test, $^{***}p < 0.0001$).

Figure S6. Effect of BgILP5 RNAi on the expression of JH biosynthesis enzymes and *Vg*. Adult *B. germanica* females were treated with dsRNA targeting BgILP5 (dsILP5) or a heterologous dsRNA (Control) during the oothecal transport period and dissections were performed on day 5 of the second gonadotrophic cycle (see Material and Methods). (A) *HMG-CoA synthase-1* (*HMG-S1*), *HMG-CoA reductase* (*HMG-R*) and *JHAMT* mRNA levels in CC-CA (n = 6-8). (B) *Vg* mRNA levels in fat bodies (n = 9-10). Y-axes indicate copies per copy of *Actin 5C*. The results are expressed as the mean ± S.E.

Figure S7. Effect of BgILP6 RNAi on the expression of *BgILPs*, JH biosynthesis enzymes and *Vg*, and on ovarian growth. Adult *B. germanica* females were treated with dsRNA targeting BgILP6 (dsILP6) or a heterologous dsRNA (Control) during the oothecal transport period and dissections were performed on day 5 of the second gonadotrophic cycle (see Material and Methods). (A) *BgILP1-6* mRNA levels in brains (n = 4-5). (B) *HMG-CoA synthase-1* (*HMG-S1*), *HMG-CoA reductase* (*HMG-R*) and *JHAMT* mRNA levels in CC-CA (n = 5-6). (C) *BgILP7* and *Vg* mRNA levels in fat bodies (n = 4-6). (D) Basal follicle length (n = 10-15). In A, B and C the Y-axes indicate copies per copy of *Actin 5C*. The results are expressed as the mean ± S.E. An asterisk represents significant differences between control and dsILP6 subjects (Student's t-test, $^{**}p < 0.005$).

Figure S8. Effect of BgILP7 RNAi on the expression of *BgILPs*, JH biosynthesis enzymes and *Vg*, and on ovarian growth. Adult *B. germanica* females were treated with dsRNA targeting BgILP7 (dsILP7) or a heterologous dsRNA (Control) during the oothecal transport period and dissections were performed on day 5 of the second gonadotrophic cycle (see Material and Methods). (A) *BgILP1-6* mRNA levels in brains (n = 5). (B) *HMG-CoA synthase-1* (*HMG-S1*), *HMG-CoA reductase* (*HMG-R*) and *JHAMT* mRNA levels in CC-CA (n = 5-6). (C) *BgILP7* and *Vg* mRNA levels in fat bodies (n = 7-10). (D) Basal follicle length (n = 8-10). In A, B and C the Y-axes indicate copies per copy of *Actin 5C*. The results are expressed as the mean ± S.E. An asterisk represents significant differences between control and dsILP7 subjects (Student's t-test, $^{*}p < 0.05$).

Figure S9. Effect of the knockdown of BgILP3, 5 and 6 on the expression of *BgILPs*, JH biosynthesis enzymes and *Vg*, and on ovarian growth. Adult *B. germanica* females were treated with dsRNA targeting BgILP3, BgILP5 and BgILP6 (dsILP3 + dsILP5 + dsILP6) or a heterologous dsRNA (Control) during the oothecal transport period and dissections were performed on day 5 of the second gonadotrophic cycle (see Material and Methods). (A) BgILP1-6 mRNA levels in brains (n = 5). (B) *HMG-CoA synthase-1* (*HMG-S1*), HMG-CoA reductase (*HMG-R*) and *JHAMT* mRNA levels in CC-CA (n = 5). (C) *BgILP7* and *Vg* mRNA levels in fat bodies (n = 4-5). (D) Basal follicle length (n = 8-9). In A, B and C the Y-axes indicate copies per copy of *Actin 5C*. The results are expressed as the mean ± S.E. An asterisk represents significant differences between control and dsILP3 + dsILP5 + dsILP6 subjects (Student's t-test, $^{*}p< 0.05$; $^{**}p < 0.005$; $^{***}p < 0.0001$).

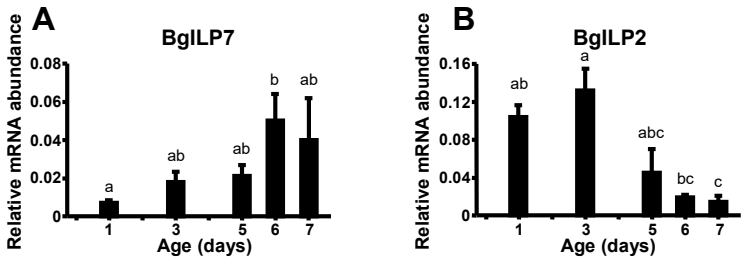
A
BgILP7
Relative mRNA abundance
0.08
0.06
0.04
0.02
0
a
ab
ab
b
ab
1
3
5
6
7
Age (days)
B
BgILP2
Relative mRNA abundance
0.16
0.12
0.08
0.04
0
ab
a
abc
bc
c
1
3
5
6
7
Age (days)

Fig. S1

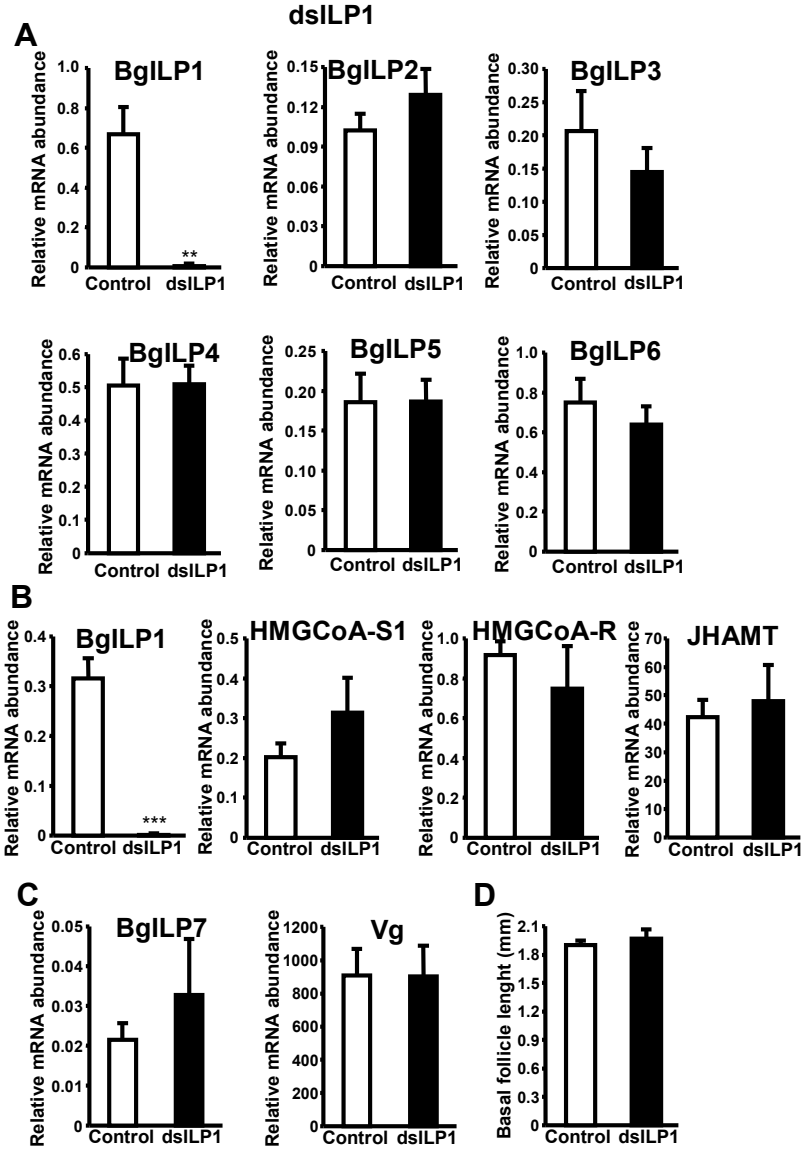
dsILP1
A
BgILP1
BgILP2
BgILP3
BgILP4
BgILP5
BgILP6
Relative mRNA abundance
Control
dsILP1
**
B
BgILP1
HMGCoA-S1
HMGCoA-R
JHAMT
***
C
BgILP7
Vg
D
Basal follicle lenght (mm)

Fig. S2

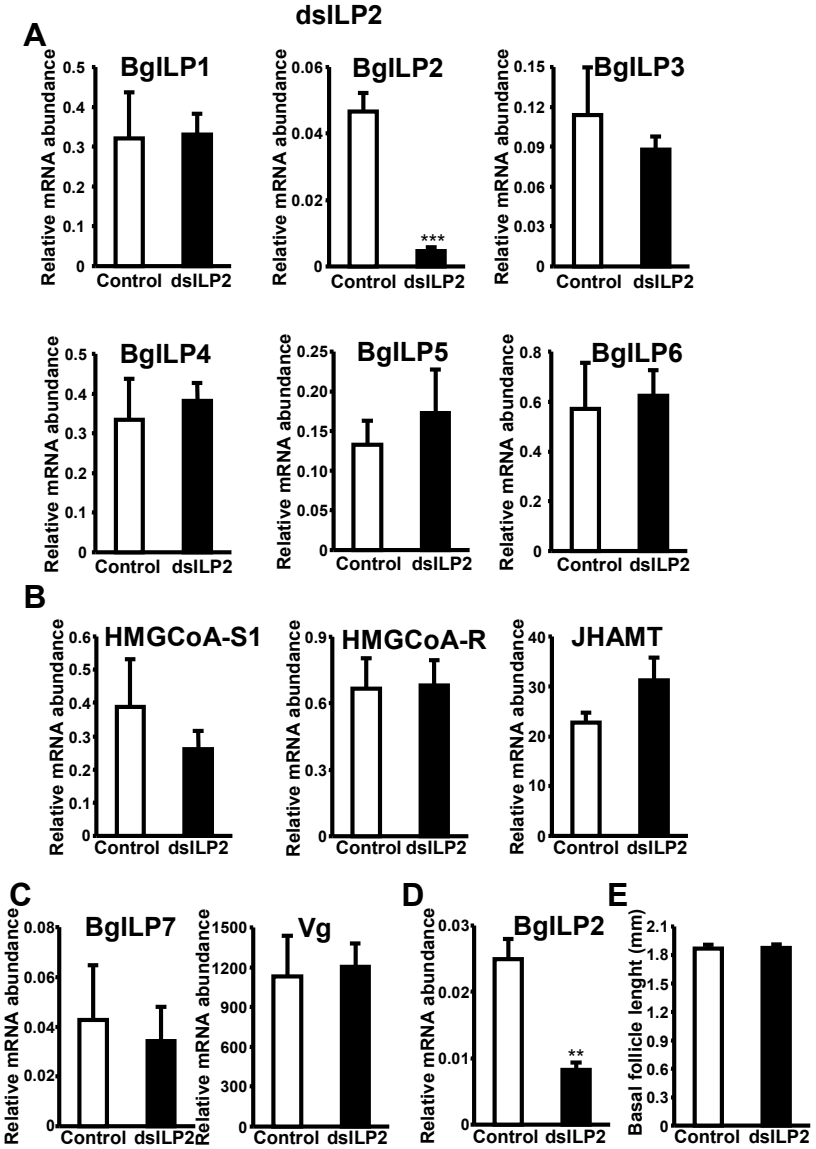
dsILP2
A
BglLP1
BglLP2
BglLP3
BglLP4
BglLP5
BglLP6
Relative mRNA abundance
Control
dsILP2
***
B
HMGCoA-S1
HMGCoA-R
JHAMT
C
BglLP7
Vg
D
BglLP2
**
E
Basal follicle lenght (mm)

Fig. S3

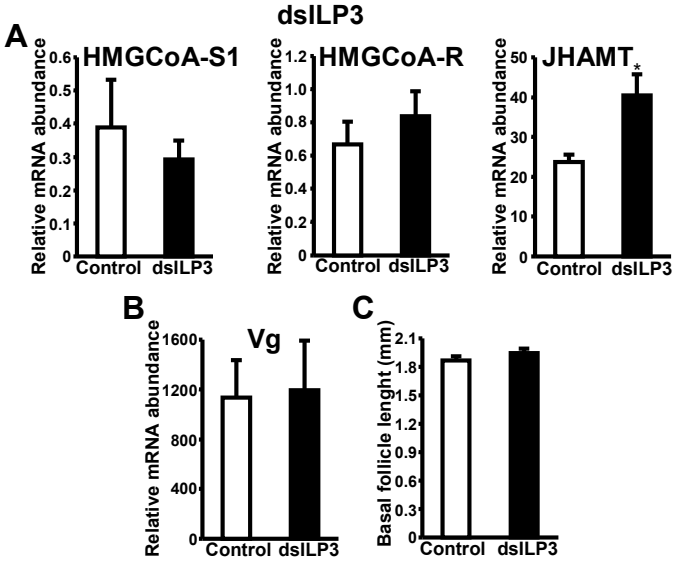
dsILP3
A
HMGCoA-S1
HMGCoA-R
JHAMT*
Relative mRNA abundance
Control
dsILP3
B
Vg
C
Basal follicle lenght (mm)

Fig. S4

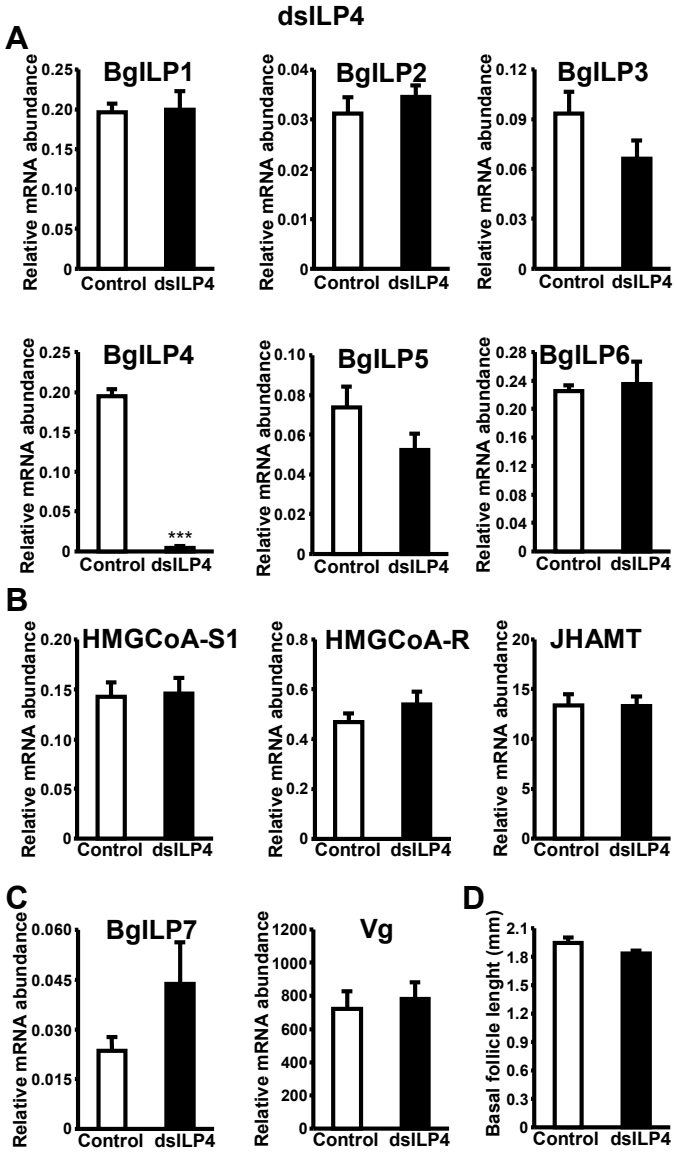
dsILP4
A
BgILP1
BgILP2
BgILP3
BgILP4
BgILP5
BgILP6
Relative mRNA abundance
Control
dsILP4
***
B
HMGCoA-S1
HMGCoA-R
JHAMT
C
BgILP7
Vg
D
Basal follicle lenght (mm)

Fig. S5

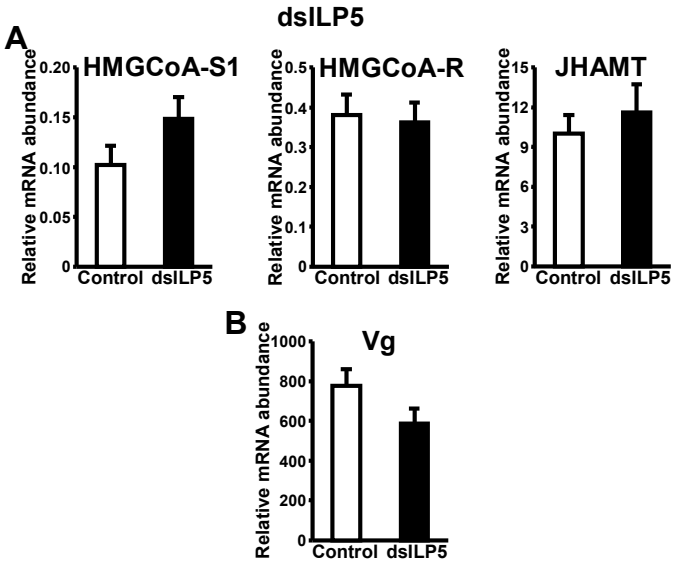
A
dsILP5
HMGCoA-S1
HMGCoA-R
JHAMT
Relative mRNA abundance
0.20
0.15
0.10
0.05
0
0.5
0.4
0.3
0.2
0.1
15
12
9
6
3
Control
dsILP5
B
Vg
1000
800
600
400
200

Fig. S6

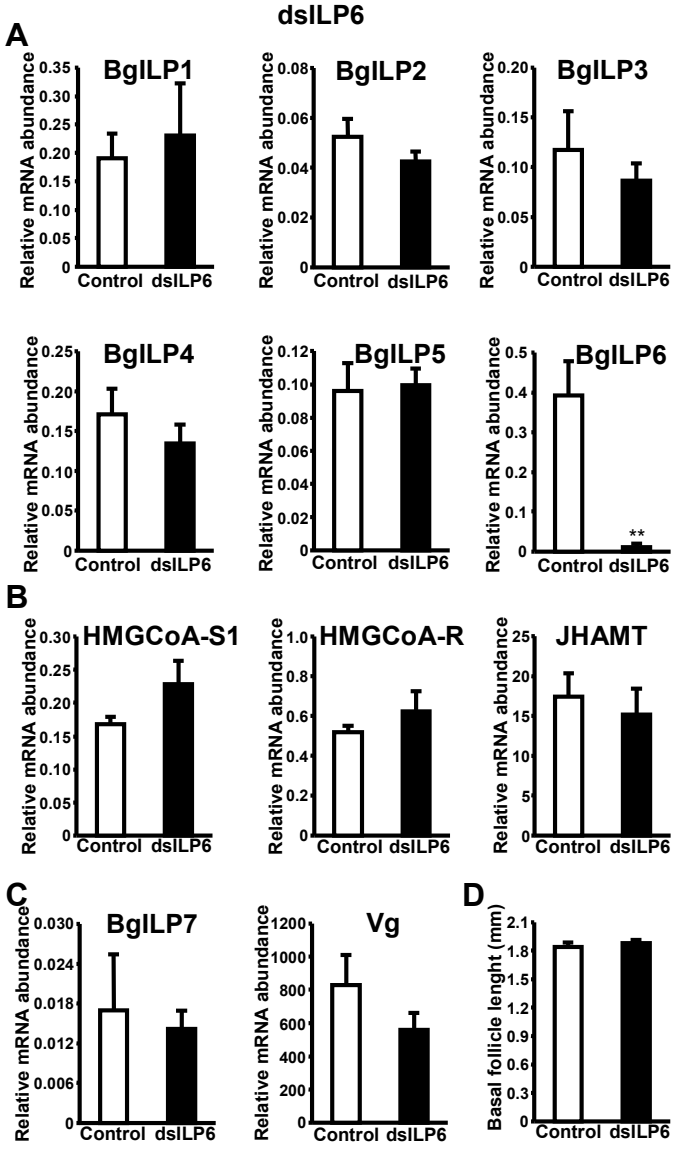
dsILP6
A
BgILP1
BgILP2
BgILP3
BgILP4
BgILP5
BgILP6
Relative mRNA abundance
Control
dsILP6
**
B
HMGCoA-S1
HMGCoA-R
JHAMT
C
BgILP7
Vg
D
Basal follicle lenght (mm)

Fig. S7

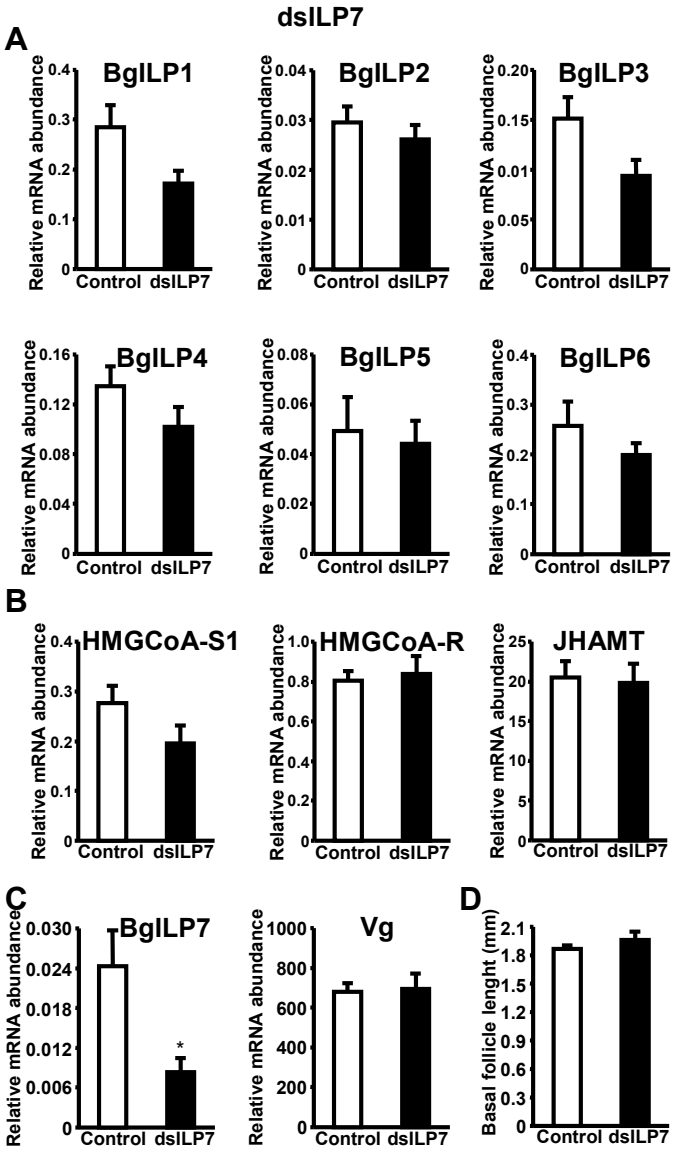
dsILP7
A
BgILP1
BgILP2
BgILP3
BgILP4
BgILP5
BgILP6
Relative mRNA abundance
Control dsILP7
B
HMGCoA-S1
HMGCoA-R
JHAMT
C
BgILP7
Vg
*
D
Basal follicle lenght (mm)

Fig. S8

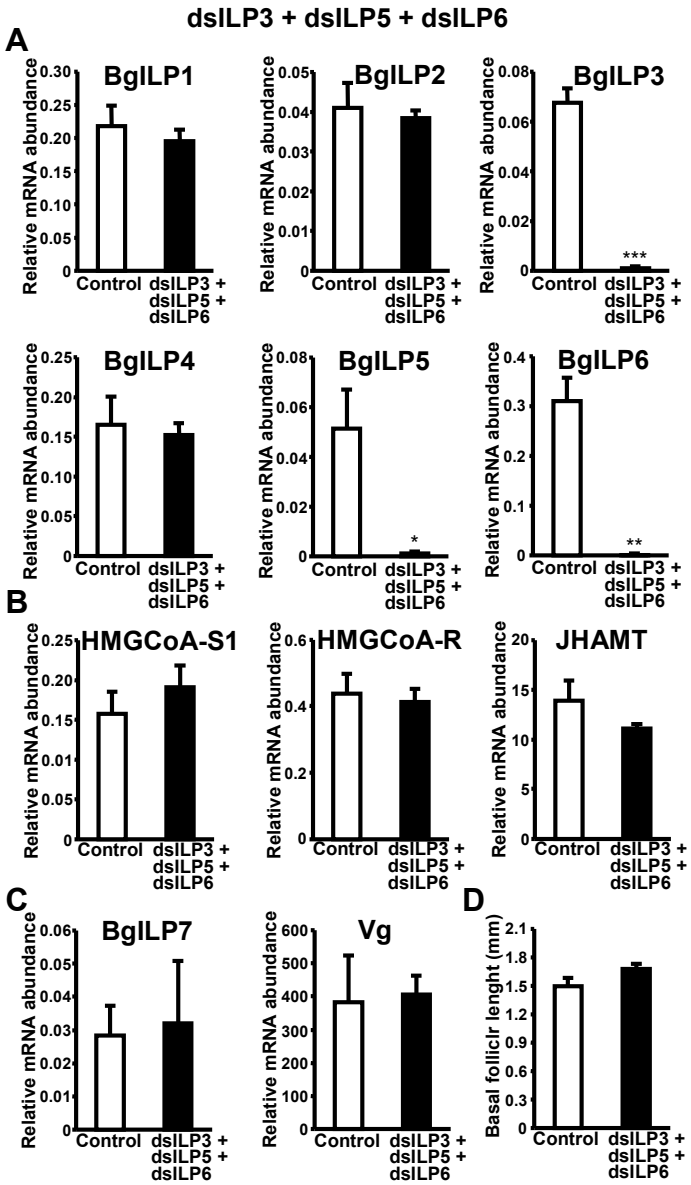
dsILP3 + dsILP5 + dsILP6
A
BgILP1
BgILP2
BgILP3
BgILP4
BgILP5
BgILP6
Relative mRNA abundance
Control
dsILP3 + dsILP5 + dsILP6
***
*
**
B
HMGCoA-S1
HMGCoA-R
JHAMT
C
BgILP7
Vg
D
Basal folliclr lenght (mm)

Fig. S9

Table S1. Primers used for qPCR.

Primer	**Sequence**
BgILP1 Fw	5′-AGAAGCAGAATTCCCTTTCCG-3′
BgILP1 Rv	5′-TCATCGACAATGCCTCCGT-3′
BgILP2 Fw	5′-TGAATGACTCGGGCTTCTGG-3′
BgILP2 Rv	5′-AGAGCTGACGCACTTGATCTTG-3′
BgILP3 Fw	5′-TGACGATTTGCTTCTCATTGTCA-3′
BgILP3 Rv	5′-CCACCAGTTTATTCCCGCA-3′
BgILP4 Fw	5′-CACTGTCAGAATCCCAATCGG-3′
BgILP4 Rv	5′-CAAATTGCATGATCTCCACCAG-3′
BgILP5 Fw	5′-GGCAAATTCATTGAAACCCAA-3′
BgILP5 Rv	5′-TTCGTTGACGGAACATCCTTT-3′
BgILP6 Fw	5′-ACACGCCTCCCGGAAATACT-3′
BgILP6 Rv	5′-ATTGCTTGGCCTTGGTGAAT-3′
BgILP7 Fw	5′-CGCCGTCATCTGGAGTTAAT-3′
BgILP7 Rv	5′-TGTCCAGAGTGCAACCTGTC-3′
HMG-CoA reductase Fw	5′-TGTGGGCAGCAGTAATTGCA-3′
HMG-CoA reductase Rv	5′-CCATCTTCCCCCCAAGGTT-3′

Table S2. GenBank accession numbers (those of BgILPs correspond to the sequences identified in the present work).

Gene	**Accession number**
BgILP1	LT984754
BgILP2	LT971386
BgILP3	LT984755
BgILP4	LT984756
BgILP5	LT984757
BgILP6	LT984758
BgILP7	LT984759
HMG-CoA synthase-1	X73679
HMG-CoA reductase	X70034
JHAMT	LT716988
Vg	AJ005115
InR	HG518668
Actin 5C	AJ862721

Table S3. Primers used for synthetizing dsRNA against the different BgILPs.

Primer	**Sequence**
BgILP1 Fw	5′-ACGGTCACAACTCATATAGAAGAG-3′
BgILP1 Rv	5′-AATTCTGCTTCTGAACCTTCTTCAA -3′
BgILP2 Fw	5′-TACATGTCATCAATTTGTAAACGCAA-3′
BgILP2 Rv	5′-AGCCCGAGTCATTCATGTCATCCAT-3′
BgILP3 Fw	5′-TATCTACAAAGGTTGCACTATAGAAG-3′
BgILP3 Rv	5′-AGTTCGTACATTTGCAACAGAAA-3′
BgILP4 Fw	5′-AACAAGGCCTCCTAGTCCTCACA-3′
BgILP4 Rv	5′-CTCTGATTTTTTCTGACTCAAGTGT-3′
BgILP5 Fw	5′-AGAGAATCTCTCGGTTACAACTG-3′
BgILP5 Rv	5′-TTCGTTGACGGAACATCCTTT-3′
BgILP6 Fw	5′-ATGAAGAACGCCTACTTGAGCCT-3′
BgILP6 Rv	5′-CCGTATCTGACTTTTTACTGGGAT-3′
BgILP7 Fw	5′-ATCATTTCGCATCCTCGACGTCT-3′
BgILP7 Rv	5′-TTTGGCTGAAAGGATCATGGT-3′